144 (2023) 213197

Contents lists available at ScienceDirect

Biomaterials Advances

journal homepage: www.journals.elsevier.com/materials-science-and-engineering-c

Assessment of thermally stabilized electrospun poly(vinyl alcohol) materials as cell permeable membranes for a novel blood salvage device

W. Joseph A. Homer [a], Maxim Lisnenko [b], Adrian C. Gardner [c,e], Eva K. Kostakova [b], Jan Valtera [d], Ivan B. Wall [e,1], Vera Jencova [b], Paul D. Topham [f], Eirini Theodosiou [a,*]

[a] Engineering for Health Research Centre, College of Engineering and Physical Sciences, Aston University, Birmingham, UK
[b] Dpt. Of Chemistry, Faculty of Science, Humanities and Education, Technical University of Liberec, Liberec, Czech Republic
[c] The Royal Orthopaedic Hospital NHS Foundation Trust, Birmingham, UK
[d] Dpt. Of Textile Machine Design, Faculty of Mechanical Engineering, Technical University of Liberec, Liberec, Czech Republic
[e] College of Health and Life Sciences, Aston University, Birmingham, UK
[f] Chemical Engineering and Applied Chemistry, College of Engineering and Physical Sciences, Aston University, Birmingham, UK

ARTICLE INFO

Keywords:
Cell salvage
Membrane chromatography
Non-woven fibres
Biomaterials
Medical devices

ABSTRACT

The use of Intraoperative Cell Salvage (ICS) is currently limited in oncological surgeries, due to safety concerns associated with the ability of existing devices to successfully remove circulating tumour cells. In this work, we present the first stages towards the creation of an alternative platform to current cell savers, based on the extremely selective immunoaffinity membrane chromatography principle. Non-woven membranes were produced *via* electrospinning using poly(vinyl alcohol) (PVA), and further heat treated at 180 °C to prevent their dissolution in aqueous environments and preserve their fibrous morphology. The effects of the PVA degree of hydrolysis (DH) (98 % *vs* 99 %), method of electrospinning (needleless DC *vs* AC), and heat treatment duration (1–8 h) were investigated. All heat treated supports maintained their cytocompatibility, whilst tensile tests indicated that the 99 % hydrolysed DC electrospun mats were stronger compared to their 98 % DH counterparts. Although, and at the described conditions, AC electrospinning produced fibres with more than double the diameter compared to those from DC electrospinning, it was not chosen for subsequent experiments because it is still under development. Evidence of unimpeded passage of SY5Y neuroblastoma cells and undiluted defibrinated sheep's blood in flow-through filtration experiments confirmed the successful creation of 3D networks with minimum resistance to mass transfer and lack of non-specific cell binding to the base material, paving the way for the development of novel, highly selective ICS devices for tumour surgeries.

1. Introduction

The blood loss associated with orthopaedic, cardiac, vascular, obstetrics and trauma surgeries often exceeds 20 % of a patient's estimated blood volume, and in cases of tumour surgeries, average losses of 2180 mL have been reported [1–3]. Despite the use of several techniques to minimize intra-operative blood loss, there is still a requirement for allogeneic blood transfusion (ABT) within modern surgical practice, with approximately 1.4 million units issued each year in the UK [4–6]. While ABT is used routinely as a life-sustaining and life-saving procedure, it is not without its own risks and complications [7]. Leading ABT-related causes of mortality include transfusion-related acute lung injury, haemolytic transfusion reactions, and transfusion-associated sepsis [8]. Based on the above safety concerns, as well as the increasing costs and ongoing variability of allogeneic blood supply, alternative solutions have been explored in the form of patient blood management (PBM) programs [9–12]. PBM can involve several practices, including preoperative autologous blood donation, red blood cell mass optimization, perioperative blood conservation and intraoperative cell salvage (ICS), all of which are designed to reduce the need for ABT and associated postoperative complications [9,11,13–16].

ICS (also known as blood salvage) is a process by which the patient's shed blood is processed during surgery to recover and then return the red blood cells back to the patient. Most commercially available ICS

* Corresponding author at: Engineering for Health Research Centre, College of Engineering and Physical Sciences, Aston University, B4 7ET Birmingham, UK.
E-mail address: e.theodosiou@aston.ac.uk (E. Theodosiou).
[1] Present address: Institute of Immunology and Immunotherapy, University of Birmingham, Birmingham, UK

https://doi.org/10.1016/j.bioadv.2022.213197
Received 13 June 2022; Received in revised form 8 November 2022; Accepted 12 November 2022
Available online 17 November 2022

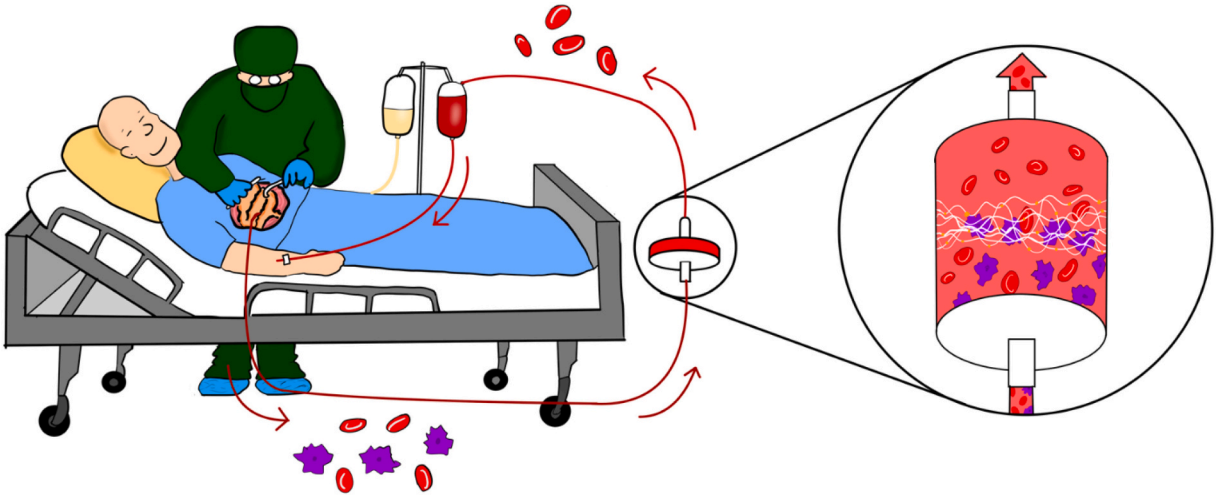

Fig. 1. Overview of the proposed cell salvage process. Blood is recovered from the patient during surgery and processed to remove tumour cells based on surface markers, before being returned to the patient. Image Copyright © 2022 Benjamin Dagès.

devices are based on centrifugation, with one device using filtration [17–21]. Whilst these separation methods can process blood quickly, they lack selectivity, and subsequently, their use in oncological surgeries poses safety concerns, with Kumar and co-workers presenting data showing the inability of the existing cell salvage devices to remove circulating tumour cells (CTCs) from blood [22]. These facts create apprehension amongst clinicians, as the reinfusion of CTCs carries the risk of metastatic spread of a primary tumour and thus failure of otherwise curative operations. CTCs are rare cells (in the order of one CTC per 10^6 white blood cells and 10^9 red blood cells per mL of peripheral blood [23]), and evidence suggests that intra-operative manipulation of a tumour during surgery can significantly increase their numbers in the blood stream [24,25]. Some publications have demonstrated successful removal, destruction, or otherwise reduction in metastatic capabilities of CTCs in salvage blood retrieved from patients undergoing primary tumour surgery, when the ICS devices were combined with leukodepletion [26–30], whilst Waters and co-workers reported no difference in the re-occurrence rate of cancer between patients receiving ABT compared to those receiving salvage blood [31]. Despite this, theoretical concern still persists within the oncological setting, with the Association of Anaesthetists recommending that the application of blood salvage in cancer surgery should be limited to case-by-case assessment and should require specific patient consent [32]. Therefore, blood recovered by ICS is not commonly employed in instances of primary tumour surgeries outside of life-or-death situations.

A potential method of overcoming the safety issues associated with the processing of blood intraoperatively, involves the development of a device which can selectively remove tumour cells, whilst maintaining the high throughput of the existing cell salvage equipment. Chromatography is widely considered as the solution to all high-resolution separation problems within the bioprocessing industry and has been used routinely in this capacity since the 1950s [33]. Amongst the different types of chromatography, immunoaffinity is the one with the highest specificity because it relies on antibody-antigen interaction, and has already been employed for lymphocyte enrichment using cell surface markers, in a similar principle to Magnetic-Activated Cell Sorting (MACS®) [34]. Cell chromatography is still in its infancy however, with macroporous monoliths being the preferred stationary phase due to their reduced resistance to mass transfer [35–37]. Stacked membranes are another chromatographic format also designed for convective flows, and therefore identified as potential material for the separation of large biological entities, such as human cells [38]. There are many different materials and configurations used for membrane chromatography supports and the reader is directed elsewhere for further details [39].

In this work, electrospinning was identified as a suitable method to create the membrane construct, because it is cost effective, fast and can produce supports with tuneable properties and geometries, while meeting the need of membranes suitable for convective flow applications [40–44]. Hardick et al. demonstrated the ability of stacked cellulose electrospun non-woven mats to achieve high throughput separations with minimal pressure drops when compared to commercially available adsorptive membranes for the processing of proteins [45,46]. Regarding the polymer of choice for the creation of the base matrix, out of the various natural and synthetic polymers that have been electrospun for biomedical applications, poly(vinyl alcohol) (PVA) seems to offer some unique advantages. PVA's biocompatible, haemocompatible and hydrophilic character renders it very popular within the medical, pharmaceutical, tissue engineering, filtration and biosensor sectors [47–54]. Additionally, PVA, which has also been described as a 'green' polymer, is inexpensive and its free hydroxyl groups can be easily functionalised using standard protocols for the immobilization of immunoaffinity ligands [55,56].

Though PVA with low (*e.g.* 88 %) degree of hydrolysis (DH) has been used extensively in electrospinning, the preparation of nanofibrous materials from >98 % DH PVA has its limitations and is dependent on the molecular weight of the polymer and the parameters of the solvent system. It is therefore necessary to optimize the composition of the polymer solution with respect to the electrospinning parameters [57–60]. Furthermore, and because PVA is a highly hydrophilic polymer which readily forms hydrogels, it is necessary to take additional steps to preserve the morphology of nanofibers and maintain the very open porous structure that is necessary for high-throughput convective flow. Electrospun PVA materials produced in literature have had their stability against dissolution improved in aqueous environment *via* different methods of crystallinity enhancement (sometimes referred to as physical cross-linking) and chemical cross-linking [47,59,61–65]. Although high molecular weight PVA with a high DH yields non-woven mats which better maintain their structure when in contact with water (compared to those created from lower DH PVA), additional stabilisation against their dissolution is still required.

Ideally, methods employed in the production of materials for biomedical applications should seek to minimize the incorporation of harmful additives (*e.g.* chemical cross-linking agents), in order to keep them safe for use in humans. Thermal treatment has shown promise in conserving the morphology of the electrospun mats by crosslinking the polymer chains without the addition of chemical agents [63,64], with the added benefit of preserving the free hydroxyl groups on the surface of the material for the attachment of immunoaffinity ligands [66].

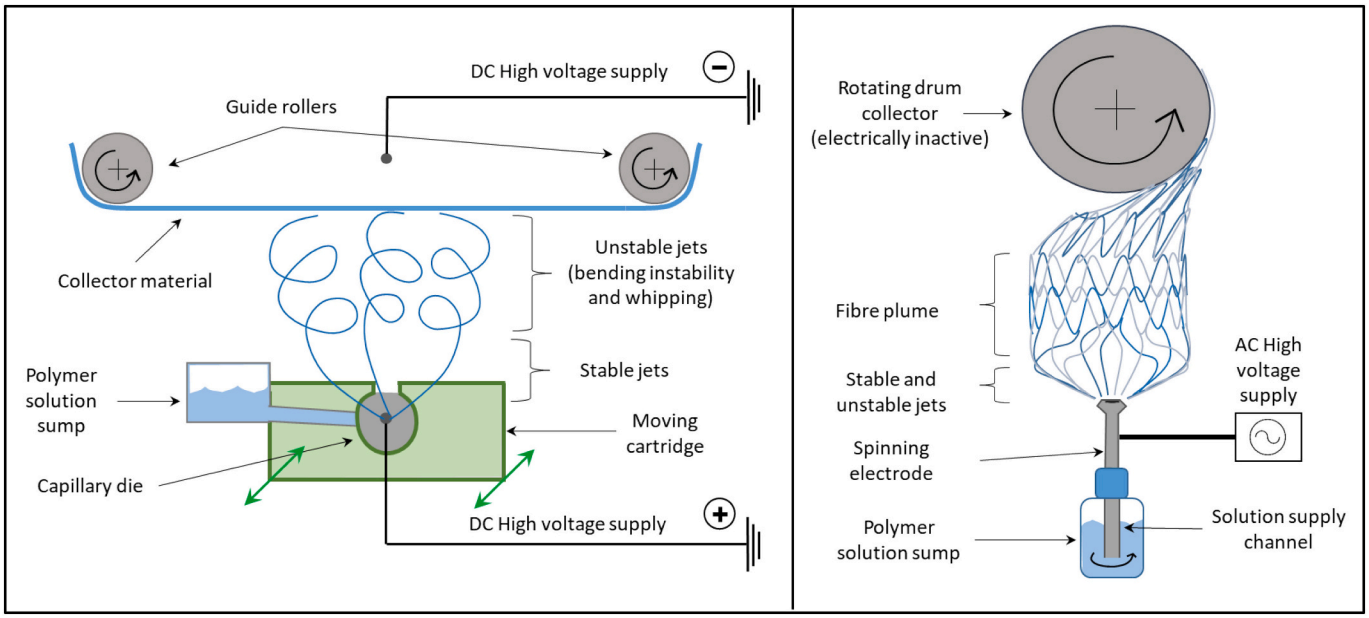

Fig. 2. Diagrams of different methods of electrospinning. Left: Wire-based configuration of needleless DC electrospinning used in the Elmarco Nanospider™. Right: AC electrospinning with rod-like electrode and rotating drum collector.

Herein, for the first time, we present initial steps towards the creation of a blood salvage device based on membrane chromatography, which has the potential to allow ICS during oncological surgery with reduced risk to the patient (Fig. 1). The device will ultimately combine the increased throughput capacity associated with the membrane format, with the high selectivity of immunoaffinity separation, and will offer a safer alternative to the existing ICS devices when used in cancer surgeries. This research investigates the effects of the degree of hydrolysis of PVA, electrospinning method and duration of heat treatment on the physicochemical characteristics of the unfunctionalized non-woven membranes, as well as their cytocompatibility and ability to allow the unimpeded cell passage through the 3D network.

2. Materials and methods

2.1. Materials

Poly(vinyl alcohol) 'Mowiol 20–98' (98 % degree of hydrolysis (DH), 125,000 M_w), PVA 'Mowiol 28–99' (99 % DH, 145,000 M_w) and Cell Counting Kit-8 (CCK-8) were purchased from Sigma-Aldrich Company Ltd. (Gillingham, UK). Ethanol (≥99.8 %) was acquired from Fischer Scientific UK Ltd. (Loughborough, UK). Dulbecco's Modified Eagle Medium (DMEM), UltraGlutamine™ and phosphate-buffered saline (PBS) were obtained from Scientific Laboratory Supplies Ltd. (Nottingham, UK). Fetal bovine serum (FBS), RPMI-1640 with L-Glutamine, and basic fibroblast growth factor (b-FGF) were purchased from Merck KGAA (Darmstadt, Germany) and PeproTech EC Ltd. (London, UK), respectively. Defibrinated sheep blood used for flowthrough testing was bought from TCS Biosciences Ltd. (Buckingham, UK). Human mesenchymal stem cells (hMSCs) were isolated from bone marrow aspirates (Lonza, Cologne, Germany) from a healthy donor after informed consent and expanded at the College of Health and Life Sciences, Aston University, UK. SH-SY5Y Neural blastoma cell line was purchased from European Collection of Authenticated Cell Culture (cat. no: 94030304) and modified for red fluorescence protein expression according to George et al., 2018 [67]. All other chemicals were purchased from Fisher Scientific UK Ltd. (Loughborough, UK).

Table 1
Electrospun samples produced in this work.

Production method	Degree of hydrolysis (%)	PVA Concentration (w/w)	Solvent ratio (dH_2O: EtOH)	Heat treatment duration (h at 180 °C)
DC	98	10 %	9:1	0
DC	98	10 %	9:1	1
DC	98	10 %	9:1	4
DC	98	10 %	9:1	8
DC	99	8 %	9:1	0
DC	99	8 %	9:1	1
DC	99	8 %	9:1	4
DC	99	8 %	9:1	8
AC	99	8 %	dH_2O	0
AC	99	8 %	dH_2O	1
AC	99	8 %	dH_2O	4
AC	99	8 %	dH_2O	8

2.2. Preparation of non-woven supports via electrospinning

Samples produced by direct current (DC) needleless electrospinning technology with wire spinning electrode (Nanospider™, Elmarco NS 1S500U; Liberec, Czech Republic), used a 50 kV voltage differential (+40 kV and -10 kV), an electrode separation distance of 16 cm, and collector material withdrawal rate of 20 mm/min (resulting in a combined electrospinning duration of ~45 min) (Fig. 2). Spinning solution (9:1 (w/w) water: ethanol solvent ratio) was applied to the positively charged electrode (wire with diameter 0.25 mm) by transversing cartridge with a capillary die diameter of 0.7 mm. Climate parameters were fixed at 22 °C (±2 °C) and 30 % (± 3 %) relative humidity by precision air conditioning unit (NS AC150, Elmarco; Liberec, Czech Republic). Samples were produced by alternating current (AC) electrospinning according to the method described by Valtera et al. [68]. Briefly, a signal generator (OWON AG1022, Owon technology, Zhangzhou, China) was connected to a high voltage amplifier (TREK 50/12C-H-CE, Advanced Energy, Denver, CO, USA) to generate a 30 Hz sinusoidal waveform, which was amplified to an effective voltage of 35 kV and supplied to a rod-like spinneret electrode with emitter diameter of 22 mm (see Fig. 2). A screw pump was used to supply polymer solution from the container

flask to the spinneret tip at flow rates of 14–18 mL/min. Nanofibers were collected on an electrically inactive drum (drum diameter 30 cm and 10 RPM rotation speed), which was placed above the electrode. The emitter-to-drum distance was 17 cm. AC samples were produced using pure water as solvent. The experiments were conducted under ambient conditions and lasted a total of 15 min per run. A spunbond nonwoven fabric (anti-static treated polypropylene non-woven, 30 g/m^2) was used as collector material during DC and AC electrospinning and for subsequent handling of the nanofiber layer. Heat treatment was carried out at 180 °C in a convection oven (SciQuip Oven-80 HT; Newtown, UK) for up to 8 h. Table 1 contains a full list of samples produced in this work and their solution parameters. All solutions were prepared by heating at 90 °C for 4 h under continuous stirring to ensure homogeneity, and then left to cool overnight.

2.3. Characterization of electrospun non-woven supports

2.3.1. Morphology

To assess fibre morphology and swelling behaviour *in situ*, ESEM images were taken using a Quattro S environmental scanning electron microscope (Thermo Fisher Scientific, Waltham, MA, USA). Examination of swelling behaviour was achieved using initial conditions of 400 Pa with a stage temperature of 2 °C. Pressure was increased gradually to 800 Pa to saturate the samples, and steadily reduced again, resulting in evaporation of surface moisture, thereby allowing observation of morphological changes. Fibre diameters were measured using ImageJ software (National Institutes of Health, Bethesda, MD, USA) and reported as an average value of no less than 113 independent measurements.

2.3.2. Chemical characterization

To investigate potential chemical changes arising from the heat treatment, Fourier transform infrared spectroscopy (FT-IR) was conducted using a Frontier Spectrometer (PerkinElmer Ltd., Waltham, MA, USA) combined with an attenuated total reflectance (ATR) accessory (GladiATR; Pike Technologies, Madison, WI, USA). Each scan was performed from 4000 cm^{-1} to 700 cm^{-1} with a resolution of 4 cm^{-1} for a total of 16 scans per measurement.

2.3.3. Crystallinity

The crystallinity of the materials was evaluated using X-ray diffraction (XRD) on a Bruker D8 Advance diffractometer, equipped with a LynxeyePSD detector (Bruker, Billerica, MA, USA) and with Cu K_α1,2 radiation (40 kV and 40 mA), 0.02 mm Ni K_β absorber, 5–50° 2θ range, a step scan of 0.02° with a sample rotation speed of 30 RPM. The degree of crystallinity was calculated using Eq. (1), where α is the degree of crystallinity, I_c is the sum of the intensity under the crystalline peaks, and I_a is the sum of the intensity under the amorphous sections of the spectra.

$$\alpha\,(\%) = \frac{I_c}{I_c + I_a} * 100 \tag{1}$$

2.3.4. Weight loss measurements

Samples of approximately 1 cm^2 (average mass 0.8 mg, $n = 3$) of each non-woven mat with controlled thicknesses, were weighed on a microbalance (Mettler Toledo XPR2, Columbus, Ohio, USA), immersed in 5 mL of de-ionized water in 7 mL glass vials and left at 37 °C for 7 days in a forced convection oven (SciQuip Oven-80 HT; Newtown, UK). Samples were subsequently dried in a vacuum desiccator overnight and then weighed once again. Weight loss percentages were calculated using Eq. (2), where W_0 is the initial weight and W_f the final weight of the sample.

$$Weight\ loss\ (\%) = \frac{W_0 - W_f}{W_0} \times 100 \tag{2}$$

2.3.5. Mechanical testing

The mechanical properties of the mats were measured by means of uniaxial tensile tests using an Instron 5965 equipped with model 2530–50 N load cell and 2712-250 N pneumatic grips (Instron, High Wycombe, Buckinghamshire, UK). The samples were prepared using a dumbbell shaped punch tool with the following dimensions: 22 mm shoulder to shoulder, 16 mm reduced section, and 4.8 mm width. Each sample (21 μm average thickness, $n = 3$) was loaded until failure (defined as a 50 % reduction from peak force) at a rate of 10 mm/min. Stress-strain curves were obtained and mean averages of the ultimate tensile strength (UTS), and strain at UTS were calculated.

2.3.6. In vitro cytotoxicity testing

The effect of potential leachables from the electrospun materials on cell viability was assessed using the extract cytotoxicity test [41]. hMSCs were seeded at 6 × 10^3 cells/cm^2 in a 96 well plate (tissue culture plastic) and cultured in cell growth medium comprising DMEM, 10 % FBS, 2 mM UltraGlutamine and 1 ng/mL bFGF, at 37 °C and 5 % CO_2 for 3 days. In parallel, electrospun mats (4 mg/mL) were added to fresh culture medium and left in the incubator for 24 h. After 3 days, the cell growth medium was replaced by the extraction liquid and incubated for another for 24 h. CCK-8 was then added to all wells and allowed to develop for 4 h as per manufacturer's protocol, before measuring the absorbance at 450 nm using a Multiskan EX plate reader (Thermo Fisher Scientific, Waltham, MA, USA). Cells cultured in the presence of 10 % (*v*/v) ethanol from day 3 were used as positive controls.

2.3.7. Flowthrough experiments using a filtration set up

Cell permeation experiments were carried out using punched electrospun discs (25 mm Ø), which were mounted in a Cole-Parmer™ filter holder. SH-SY5Y neural blastoma cells were seeded at 25 × 10^3 cells/cm^2 in RPMI-1640 cell culture medium containing 10 % FBS, expanded until confluent, harvested in PBS and adjusted to a concentration of 10^7 cells/mL for flowthrough experiments. Routinely, 4 mL of this cell suspension (total challenge of 4 × 10^7 cells) were passed through the membrane at a flow rate of 6 mL/min using a syringe pump (AL-1800, WPI, Sarasota, FL, USA), followed by two washes with PBS (2 mL under standard flow, and then 1 mL under reverse flow), with 1 mL fractions being collected throughout. Finally, 2 × 10 mL washes at 60 mL/min under standard and subsequently reverse flow were carried out to purge any remaining cells in the system, and 10 mL fractions were collected. The total membrane thickness averaged 18 μm, resulting in a bed volume of 8.8 μL. Further flowthrough experiments challenged stacked membranes (average membrane thickness of 110 μm, and total bed volume of 54.0 μL) with 5 mL of undiluted defibrinated sheep's blood, followed by two PBS wash steps (45 mL under standard flow and 5 mL under reverse flow). Fractions of 5 mL were collected throughout the experiment. Cell counts were carried out on all fractions using a Bright-Line haemocytometer (Sigma Aldrich, Gillingham, UK).

2.4. Statistical analysis

Statistics for histogram data was calculated using Microsoft Excel version 2205 with a confidence interval of 95 % to produce mean and standard deviations. All other data is presented as a mean ± standard deviation for error bars ($n = 3$). FT-IR data was normalised by trace matching the associated CH peak at 2920 cm^{-1}.

3. Results and discussion

This work explores electrospun non-woven mats based on PVA as cell permeable matrices arranged in a membrane chromatography format. First, samples produced by scale-flexible needleless DC electrospinning using stock material of 98 % and 99 % DH PVA were subjected to a series of heat treatments and compared against each other in terms of morphology and material stability. Based on these results, a single

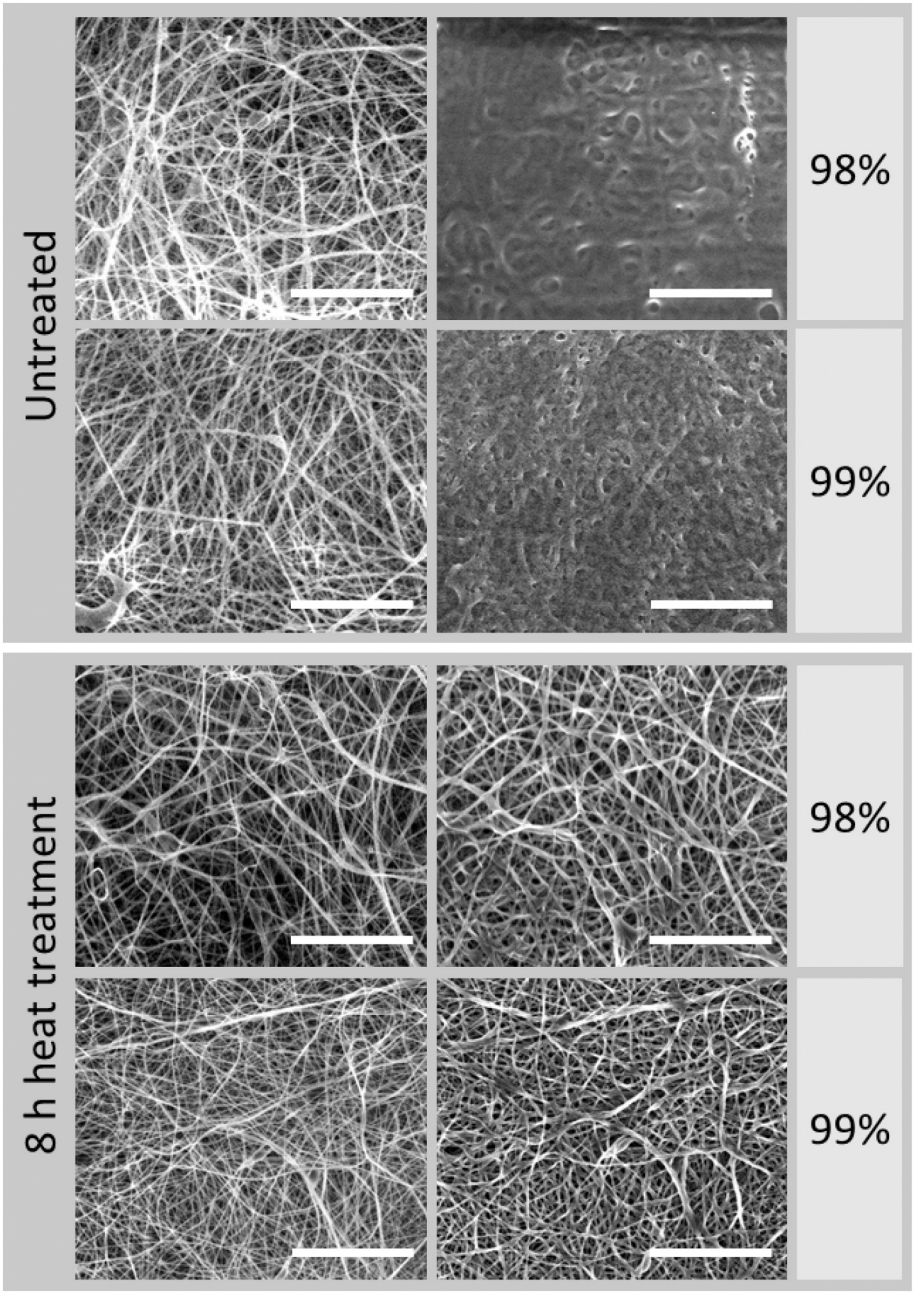

Fig. 3. ESEM images of electrospun PVA samples with 98 % and 99 % DH, produced by DC electrospinning. Left: Samples prior to swelling. Right: Samples after swelling, immediately following surface moisture evaporation. Scale bar: 30 μm.

starting feedstock (99 % DH) was used as a basis to explore differences in morphology arising from two different electrospinning setups and methods (DC and AC electrospinning), focusing on chemical comparisons of the base materials and those arising from heat treatment, as well as cytocompatibility issues. Additional extrinsic factors relating to scalability, suitability and sample handling limitations associated with each production method, were also considered when choosing the most suitable technique for subsequent experiments. Since ultimately the material must allow the free passage of blood cells across the membrane, flowthrough testing was carried out on candidate non-woven membranes to assess transmembrane penetration of cell suspensions.

3.1. Effect of PVA degree of hydrolysis and heat treatment on the creation of insoluble non-woven mats

Samples of both 98 % and 99 % PVA produced by DC spinning and heat treated at 180 °C for durations ranging from 0 to 8 h were analysed by ESEM to observe their morphology and swelling behaviour as the samples become saturated with dH_2O, and examine the ability of each sample to retain said morphology after an initial absorption phase. Prior to contact with water, all materials show a fibrous morphology with few defects present (Fig. 3 and S1 left-hand column). As expected, following hydration (Fig. 3 and S1 right-hand column), fibres not subjected to heat treatment were not able to retain their initial morphology, though the degree of swelling and blending into an amorphous structure was less pronounced in the 99 % DH samples than those from 98 % DH PVA. Heat treatment for 8 h appears to have successfully preserved the morphology

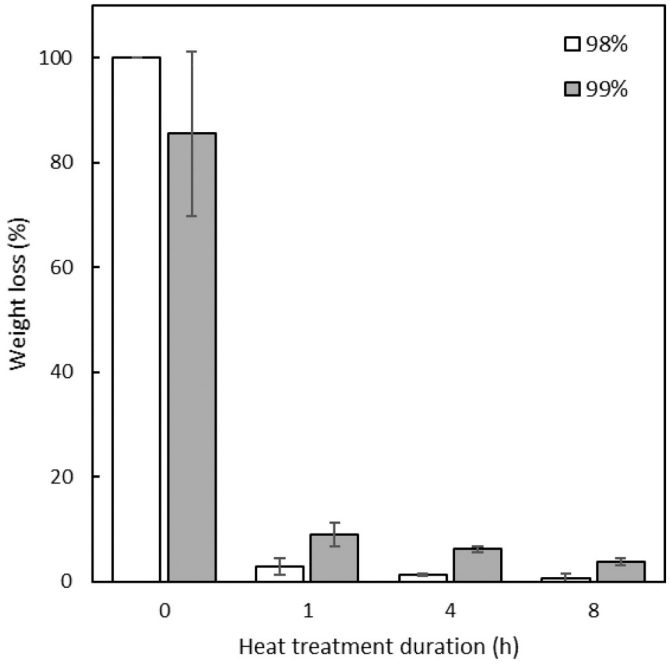

Fig. 4. Weight loss of DC electrospun PVA mats produced using different heat treatment durations, following 7 days immersion in water at 37 °C ($n = 3$). Key: 98 % DH (white); 99 % DH (grey).

of the fibrous network irrespective of the PVA degree of hydrolysis. This agrees with literature findings, which attribute this to an increase in physical crosslinking as a result of closer packing of the polymer backbone and subsequent increase of hydrogen bonding [63,64]. Close inspection reveals that the thinner fibres of the 98 % DH sample are more swollen compared to those of the 99 % one, or potentially coalesce due to surface tension created by the surface moisture. This suggests that within the described production parameters, the higher degree of hydrolysis can be advantageous in the creation of a stable non-woven structure, since it maintains an unaltered open pore configuration upon hydration, which is essential for the free passage of cells through the membrane.

The effectiveness of the heat treatment in the creation of insoluble fibres was quantified by weight loss measurements and the results are presented in Fig. 4. In addition to preserving the original fibrous network for optimal operation during blood salvage, the potential presence of leached polymer because of dissolution, presents a concern, as this may have implications in the safety of the proposed technology and prohibit regulatory approval. The 98 % DH samples without heat treatment dissolved completely after a week of water immersion, whilst a small amount of material remained in the equivalent 99 % DH samples. The latter, however, lost its initial membrane structure and formed globules upon removal from the water, thereby making it extremely difficult to handle. Any heat treatment (as low as 1 h) resulted in substantially reduced weight loss, and therefore leaching, and there was a clear correlation with the length of heat treatment in both sample series and the extent of weight loss. The 98 % DH supports lost only 0.6 % of their initial weight following the longest treatment *c.f.* 3.8 % for the 99 % DH samples, which is somewhat against expectations based on swelling and morphological assessments. In both cases however, the total loss is very small, and not deemed prohibitive for the use of these materials for cell salvage applications, which will routinely last for a few hours rather than days.

Any membrane utilized within a blood salvage device will be subject to stresses induced by cross membrane flow. Therefore, tensile tests were performed to assess the mechanical strength between supports produced from each stock material and the subsequent effects of heat treatment (Fig. 5; refer to Table S1 for a complete set of data). Samples produced from 99 % DH PVA appeared significantly stronger than those created from 98 % DH PVA, with untreated samples having 62 % greater UTS (4.68 MPa for 99 % DH *c.f.* 2.88 MPa for 98 % DH), most likely due to the reduced chain mobility, as a result of fewer acetate groups and increased hydrogen bonding. This was also observed within a polymer blend by Restrepo et al., where it was shown that PVA with higher degree of hydrolysis resulted in stronger materials [69]. Strength differences in heat treated mats were 20–25 % greater in the 99 % DH sample than the equivalent 98 % samples, with 98 % hydrolysed samples achieving UTS at 5.82 MPa (1 h), 5.33 MPa (4 h), and 5.23 MPa (8 h), compared to UTS of 6.98, 6.67, and 6.67 MPa for the respective pairs from 99 % hydrolysed PVA. This is attributed to the lack of steric hindrance caused by a decrease of the large acetate groups in the 99 % hydrolysed PVA, and the formation of strong hydrogen intramolecular

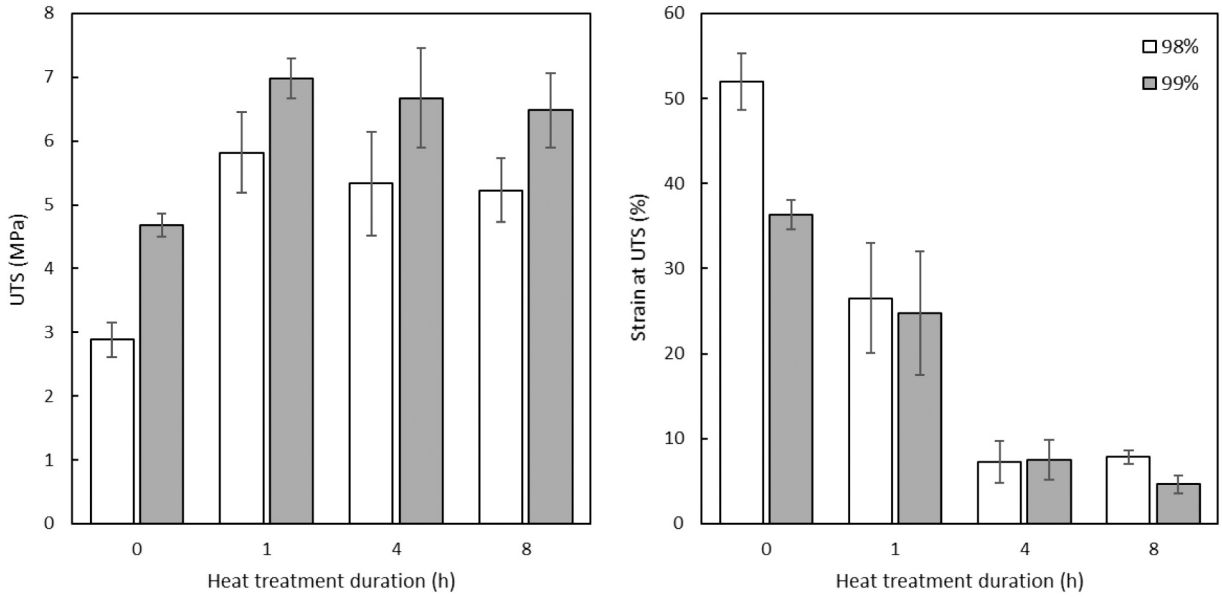

Fig. 5. Tensile performance of PVA mats produced by DC electrospinning following a range of heat treatment durations. ($n = 3$). Key: 98 % DH (white); 99 % DH (grey).

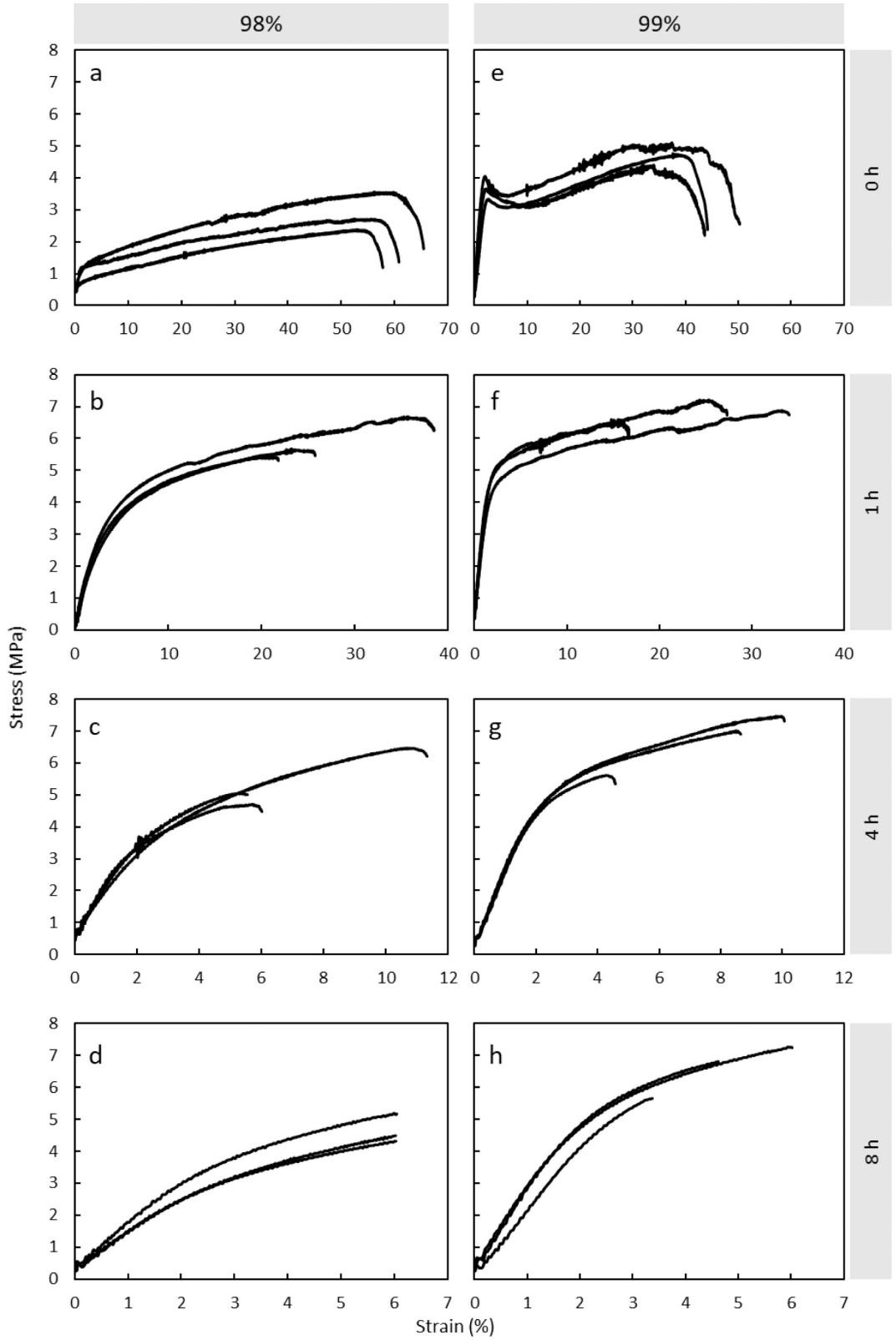

Fig. 6. Stress-strain graphs of PVA mats produced by DC under tensile load. Left column: 98 % DH samples heat treated for 0, 1, 4 and 8 h [a-d]. Right column: 99 % DH samples heat treated for 0, 1, 4 and 8 h [e-h].

bonds leading to increased ordering of the polymer chains and more effective chain packing. Heat treatment can further enhance the crystallinity of PVA and lead to stronger supports [70]. The subsequent steady reduction in material strength may be associated with a combination of increased crosslinking (both physical and potentially chemical, see Section 3.2), increasing brittle behaviour, and a slow thermal degradation effect, which can result in some chain scission and formation of polyenes (suggested by visual discolouration, as shown in

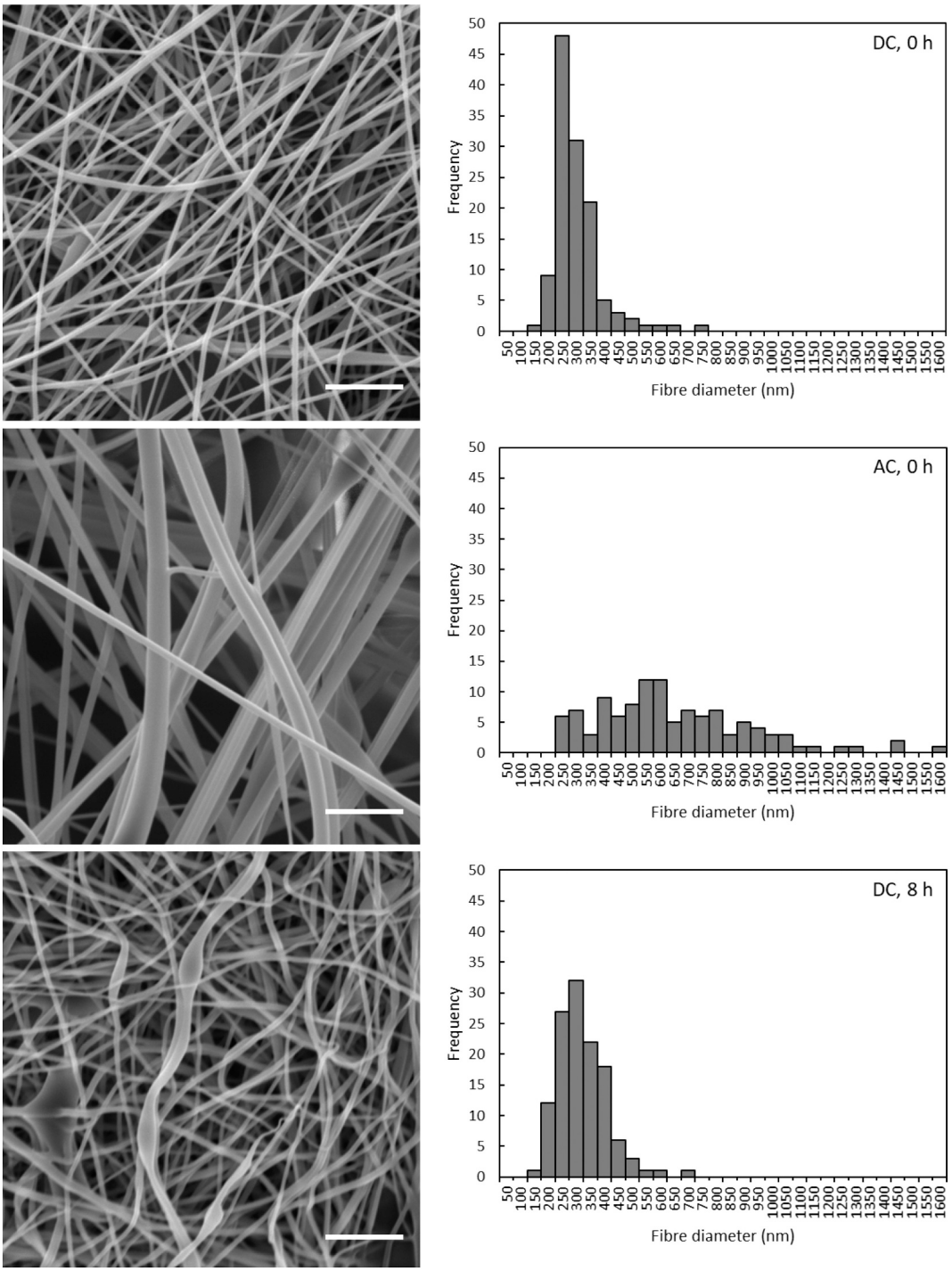

Fig. 7. SEM images and accompanying histograms comparing fibre diameter distribution of untreated electrospun 99 % DH PVA materials produced by DC and AC electrospinning, as well as a non-woven mat produced by DC electrospinning and treated for 8 h after water immersion. SEM scale bar: 5 μm.

Fig. S2) [71]. Conversely, and due to differences in chain mobility, untreated 98 % DH samples tolerated strain which was on average 15.6 % greater than the 99 % DH untreated mats, while treated versions of both sample series performed quite similarly across all durations (average strain at UTS of 25.7 %, 7.4 %, and 6.2 % for 1 h, 4 h and 8 h heat treatments; see Table S1). These small differences (0.3 %–3.2 % between paired samples) can be explained by variation in the rate of crosslinking, influenced by the ease of packing of the polymer chains and subsequent rate of formation of hydrogen bonds. Comparison of the supports treated for 0 and 1 h shows signs of a typical strength-ductility trade off [72]. The further reduction in ductility of the non-woven mats treated for 4 and 8 h (not associated with increases in strength) may also be attributed to a combined effect of reduced chain mobility through crosslinking and an increasing degree of chain scission, as it was noted that heat treatment beyond 8 h can cause the material to become excessively brittle during handling.

Despite the popularity of electrospun materials in areas such as tissue engineering and drug delivery, their use in bioprocessing applications is rarely reported and therefore it is difficult to make direct comparisons between the mechanical properties of the membranes created in this work and published data. For example, UTS values between 3 and 106 MPa have been quoted for electrospun nanofibres, depending on the

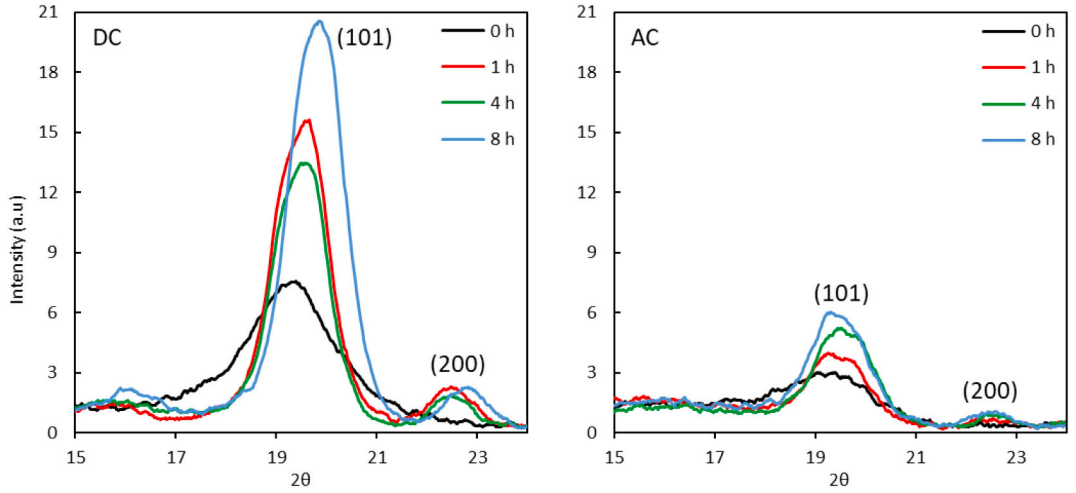

Fig. 8. XRD spectra of 99 % DH PVA materials produced by DC electrospinning (left) and AC electrospinning (right). Key: 0 h (black), 1 h (red), 4 h (green), and 8 h (blue).

polymer and the medical application [73]. Dods and co-workers produced non-woven cellulose nanofibers for ion exchange chromatography of proteins [74], an application very similar to cell separation, and their measured UTS values of 5–14 MPa are in the same region as the numbers obtained in this work.

To convey the character of each material's behaviour, stress-strain curves for all samples are shown in Fig. 6. Of all the samples, only the untreated 99 % DH ones exhibited a clear yield point followed by strain softening (Fig. 6e), commonly associated with more ductile materials [75]. This sample also features an elastic region reaching much greater stress before its yield point, when compared to its 98 % counterpart. Other profiles (Fig. 6b-d and f-h) demonstrate the tough and strong character commonly associated with plastics, with increasing heat treatment duration resulting in more sudden brittle failures in both sample series.

3.2. *Effect of the electrospinning method on the creation of the non-woven mats*

Given the enhanced preservation of the fibre morphology and greater material strength observed in the 99 % DH sample series, this material was taken forward for further research into the influence of the electrospinning method on material properties, using mats produced by the already established needleless DC technology and the more novel AC platform.

Examination of the materials by SEM (Fig. 7, top and middle) showed that both electrospinning methods were able to produce non-woven mats, with minimal occurrence of defects and highly fibrous morphology. The supports created by AC electrospinning have much thicker fibres compared to those made by DC, measuring average widths of 624 nm (±51 nm, CI = 95 %, n = 113) and 280 nm (±15 nm, CI = 95 %, n = 124), respectively. DC electrospinning also produced a much narrower size distribution with a positively skewed modal distribution, whereas the AC samples were more evenly dispersed across a broader range with no significant mode. Furthermore, the SEM image and accompanying histogram of post-water immersion DC spun PVA after 8 h of heat treatment (Fig. 7, bottom) shows a distribution very similar to the untreated supports, but with a higher average fibre width of 296 nm (±16 nm, CI = 95 %, n = 124) attributed to a small degree of swelling, indicating the heat treatment does not negatively impact fibre morphology.

XRD analysis was employed to identify differences in crystal structure, or chain ordering, between the mats and as a result of the thermal annealing process, with the (101) and (200) peaks (Fig. 8) representing

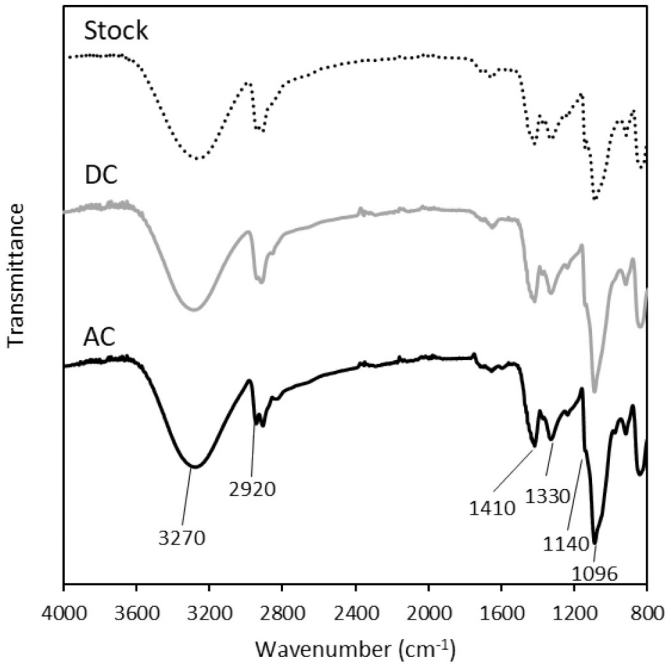

Fig. 9. FT-IR Spectra of 99 % DH PVA stock film (dotted line), and materials produced by DC (grey line) and AC electrospinning (black line) with vertical offsets for clarity.

the reflections of monoclinic unit cell [62,76]. The untreated samples from DC and AC electrospinning had a degree of crystallinity of 48.68 % and 34.64 % respectively. The overall trend indicates increased crystallinity with extended thermal treatment duration, with the highest crystallinity found in samples treated for 8 h (58.46 % for DC spun samples and 39.68 % for those produced by AC). This may be influenced by other factors including solvents used and differences in ambient production conditions, but also may be driven by the technology itself. The lack of a grounded collector in AC electrospinning may result in samples with lower degrees of ordering, as crystallinity has been found to be influenced by the strength of the attractive force between the origin of the polymer solution and the collector [77]. This increase is associated with reduced swelling and solubility of PVA and should result in a reduction in material leaching and more stable morphology, corroborating the results presented in Section 3.1.

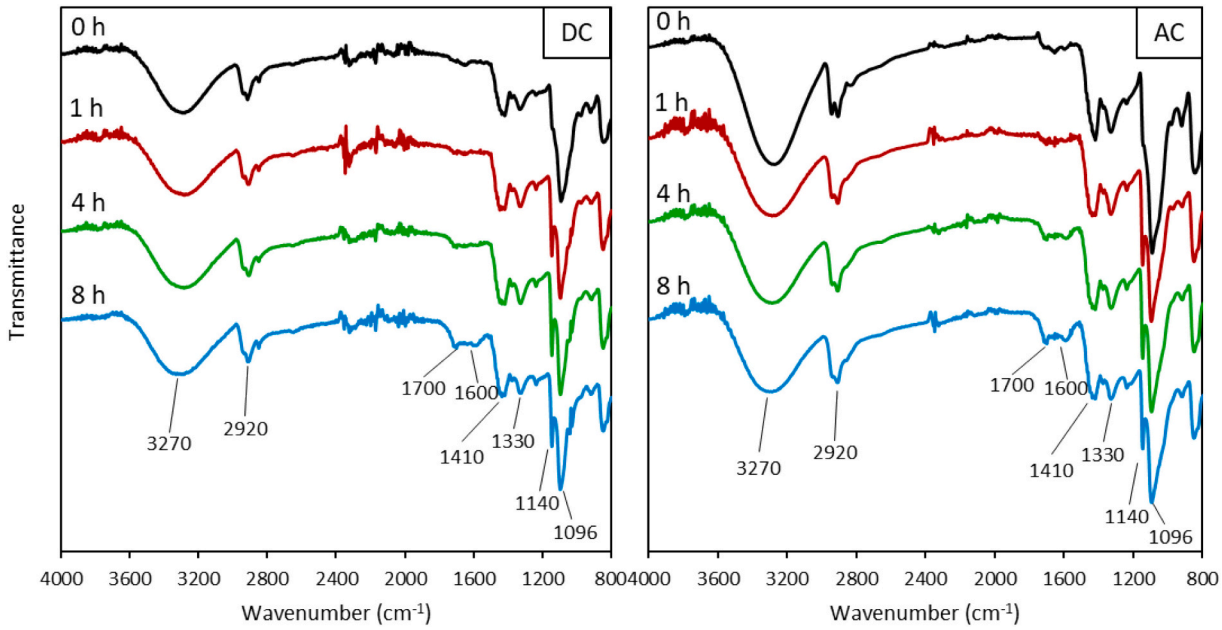

Fig. 10. FT-IR Spectra of two sample series of 99 % DH PVA produced by DC (left) and AC (right) electrospinning with heat treatment time points indicated on the offset spectra.

In addition to crystallinity, the materials were studied for any chemical differences arising from the electrospinning processes, and the FT-IR spectra of the non-woven fibres produced by the needleless DC and the AC equipment are presented in Fig. 9. The characteristic peaks of the spectra are associated with O—H stretching at 3270 cm^{-1}, C—H stretching on the polymer backbone at 2920 cm^{-1} and vibration at 1410 cm^{-1}, C—O stretching at 1140 cm^{-1} (attributed to the crystalline phase of PVA) and vibration at 1330 cm^{-1}, C═O stretching (from residual acetate groups) and O—H bending at 1096 cm^{-1} (attributed to the amorphous phase) [62,78,79]. The spectra show little difference between samples and their character is closely matched by spectra of both pristine and electrospun PVA samples with high degree of hydrolysis found in the literature [62,78,80]. An increased intensity of the band at 1096 cm^{-1} in the electrospun samples compared to the stock film is likely attributable to O—H bending associated with less ordered materials.

The effect of heat treatment on the materials was also analysed by FT-IR (Fig. 10). All heat treatments of samples produced by DC and AC cause a significant increase in peak intensity around 1140 cm^{-1}, most likely indicating the increase in crystallinity, as shown within the XRD data. In AC electrospun mats, heat treatment of any duration caused a stepwise change in intensity around 3270 cm^{-1}, which might indicate a reduction in O—H bonds, though a strong signal was still observed, suggesting that hydroxyl groups were still present in all samples. The reduction in this band, coupled with the increase and maintenance of the signal strength around 1140 cm^{-1}, may indicate that chemical cross-linking is occurring in the form of ether bonds, as C-O-C bonds share wavelengths with C—O stretching of alcohol groups. This explains the extent of reduction in solubility and preservation of the fibrous morphology observed in heat treated samples [81,82]. Finally, more extensive heat treatments (4 and 8 h) begin to show clear signals around 1600 and 1700 cm^{-1}, which are associated with formation of C═C and C═O bonds, respectively [83]. This suggests there is also degradation due to thermolysis over time, resulting in chain scission and the formation of polyenes [71]. These data support earlier mechanical testing results, where crystallinity changes may initially contribute to gains in material strength, while subsequent losses in strength correlate with a reduction in chain lengths and thus chain entanglement, as well as other structural changes to the polymer backbone.

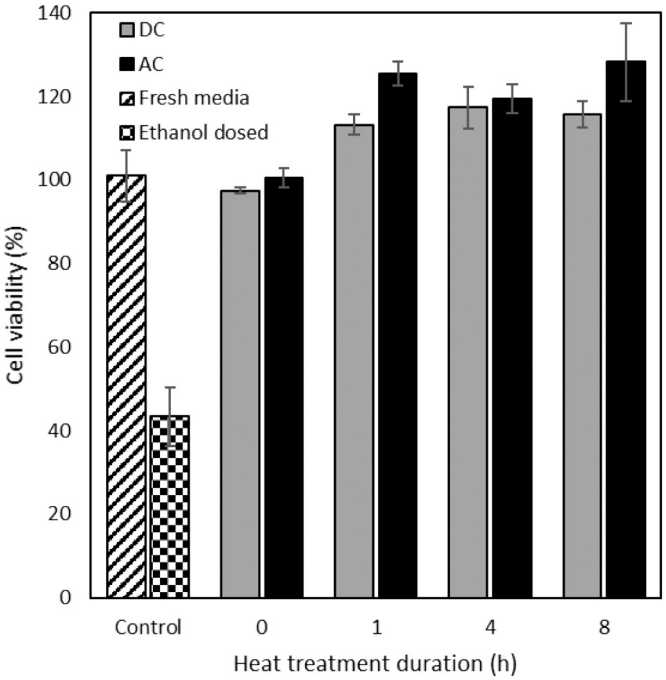

Fig. 11. Cytotoxicity of 99 % DH PVA materials produced by DC and AC electrospinning following heat treatment between 0 and 8 h, using hMSCs measured with the CCK-8 assay. Key: Fresh medium control: hatched; Ethanol control: chequered; DC: grey; AC: black.

3.3. Cytotoxicity of the non-woven mats

Cytotoxicity testing of the DC and AC spun membranes was carried out, to examine the effects of the two electrospinning methods and heat treatment durations on the cytocompatibility of the otherwise highly biocompatible PVA (Fig. 11 and Figs. S4 & S5). The extract method was chosen for these tests because it is the most adopted protocol for the *in vitro* cytotoxicity evaluation of medical devices, as it can be applied to a wide range of materials that may leach toxic substances from exposed

Table 2
Comparison of the material configurations and manufacturing considerations when DC needleless and AC platforms are used for the electrospinning of the PVA supports.

	DC Electrospinning	AC Electrospinning
Material format	Sheet/membrane configuration	Loose fibres, akin to highly sparse sheet-insulation, with tuneable micro and macro structures
Fibre and effective pore size	Smaller diameter fibres with a tight size distribution Smaller effective pore size	Larger diameter fibres with a broad size distribution Larger effective pore size [86]
Scalability	Mature technology Readily scalable (from laboratory to high volume manufacturing) Highly reproducible	Novel technology still under development
GMP potential	Semi-industrial machinery that can be incorporated into a GMP process relatively easily	Difficult to incorporate into a GMP process due to poor environmental controls in current set ups and subsequent variability of output

surfaces [84]. The extraction time used in this work was 24 h, which significantly exceeds the anticipated contact time (<1 h) of the membranes with biological fluids when in use for blood salvage. The dissolved untreated mats had almost no effect on cell growth when compared to the fresh medium control sample, whilst medium conditioned with all other samples resulted in an increase in cell metabolic activity ranging between 13 and 17 % for the DC and 20–28 % for the AC. Although there seemed to be no clear trend with respect to the duration of the heat treatment, the results are highly reproducible and confirm that any leachables from the potential dissolution of PVA have no cytotoxic effect under these conditions. This is a very promising result when considering the final application of the mats in cell-contacting medical devices, irrespective of production method and heat treatment duration.

3.4. Material selection for blood salvage devices

When selecting materials for the creation of medical devices, such as this one for blood salvage, in addition to material properties and cell compatibility, fibre configurations and manufacturing issues should also be taken into consideration (see Table 2). The non-woven mats produced by each method are quite distinct in form. Samples from DC needleless spinning are manufactured as large sheets that are lightly adhered to a spunbond fabric support, thereby making them easy to lift, transport and handle, and practically resulting in zero loss of material. In stark contrast, all samples produced in the AC equipment appear very similar to a loose sheet-insulation configuration, which can snag, stretch and

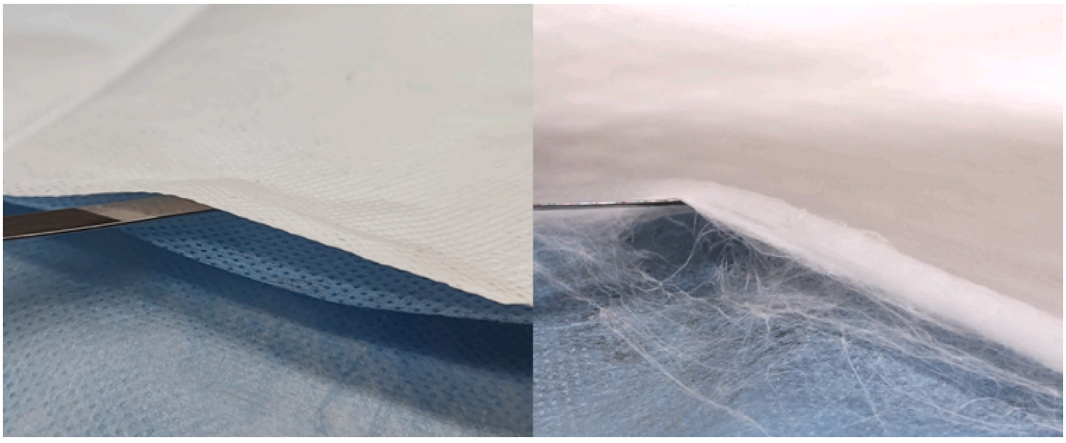

Fig. 12. Image of PVA materials produced by DC (left-hand side) and AC (right-hand side) electrospinning being lifted from the spunbond substrate.

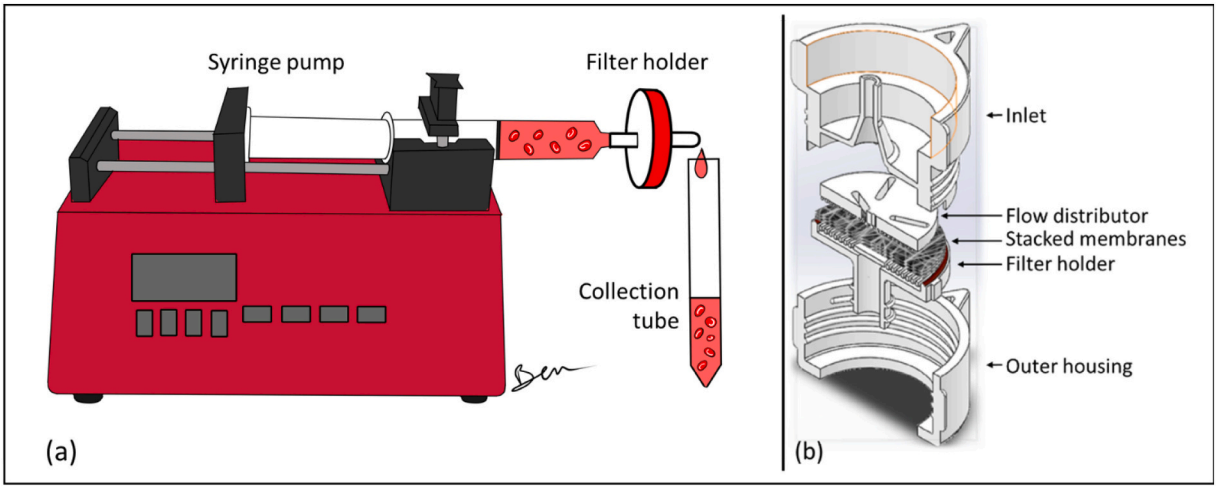

Fig. 13. (a): Illustrated setup of the flowthrough experiment. Flow of cell suspensions was achieved using a syringe pump under constant flow through a filter holder containing the electrospun membranes. Fractions were collected at the outlet of the filter holder. (b): Cross section of the exploded filter holder assembly including the nanofiber membrane support. Image (a) Copyright © 2022 Benjamin Dagès.

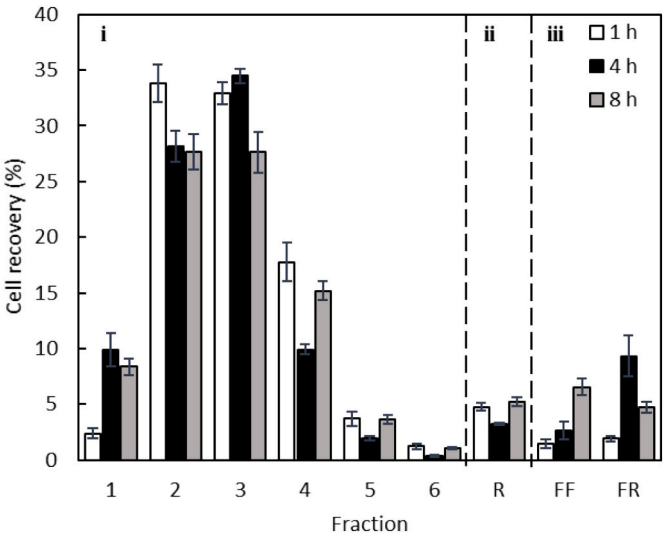

Fig. 14. Percentage of SH-SY5Y cells recovered per fraction following flow-through experiments using heat treated 99 % DH PVA materials produced by DC electrospinning. Phase i: collected fractions representing initial cell challenge of 4 mL of suspension at 10^7 cells per mL (6 mL/min flow rate), followed by PBS wash. Phase ii: PBS reverse wash fraction (fraction R). Phase iii: forward (fraction FF) and reverse (fraction FR) wash steps at 60 mL/min, used to purge loose cells from the system. (Phase i and ii fraction volume: 1 mL; phase iii fraction volume: 10 mL). Key: 1 h heat treated membranes (white); 4 h (black); 8 h (grey).

aggregate, if not handled with extreme care (Fig. 12). In its current state, AC electrospinning suffers from some drawbacks in terms of handling and ease of manufacture, and the technology is still at a development phase even at laboratory scales, which poses barriers to its use for clinical applications. On the other hand, however, the high effective pore size of the AC supports (as can be seen in Fig. 7) could be viewed as a major advantage in the processing of large human cells, as it will allow their unimpeded passage and minimize mechanical entrapment. Whilst cell size may be an issue for the majority of cell separation applications, the use of this material in blood processing only requires penetration of suspended particulates <10 μm, which matches the profile of the key cell population, *i.e.* human RBCs [85].

Though there are clear benefits to the fibre morphology and overall structure of the samples produced by AC electrospinning, the technology is not yet developed as a production platform and is only being utilized at lab-scale for research purposes. When considering both scalability and the ability for easy adaptation into GMP, the commercial maturity of the needleless DC technique utilized in the Nanospider™ and similar devices, provides key advantages for both scale-up and scale-out potential, with large semi-industrial equipment already available on the market, such as the Elmarco NS 8S1600U, featuring 8 electrodes, each 1.6 m long [87]. Furthermore, the design of these machines includes internal climate controls in a relatively closed system, whereas existing AC research typically does not feature such capabilities, which limits reproducibility. Therefore, and although preliminary AC results are extremely promising, subsequent experiments involving cell permeation studies through the membranes, were carried out with the DC electrospun mats.

3.5. Cell permeation

To demonstrate the successful unimpeded flow of cells through the PVA non-woven mats produced with DC electrospinning equipment, flowthrough experiments were setup as shown in Fig. 13(a) with membranes placed within the filter holder as shown in Fig. 13(b). The flow rate of cell suspensions was held constant at 6 mL/min during cell challenges and wash steps, with very brief pauses between each collected fraction. This flowrate provides a superficial fluid velocity of 0.02 cm/s, which closely matches the flow velocities found in capillaries, therefore providing the minimum design base for operating conditions in a clinical setting. The membranes used in all experiments were 99 % hydrolysed DC electrospun PVA materials which were thermally stabilized for 1, 4 and 8 h.

Freshly harvested SH-SY5Y cells were suspended in PBS at a concentration of 10^7 cells per mL, and 4 mL of this suspension was passed through the membrane, followed by washing steps with PBS, to assess the ability of the cells to permeate the membrane under the given conditions (Fig. 14). The cells collected in each fraction are shown as a percentage of total cells recovered. A consistent breakthrough effect was

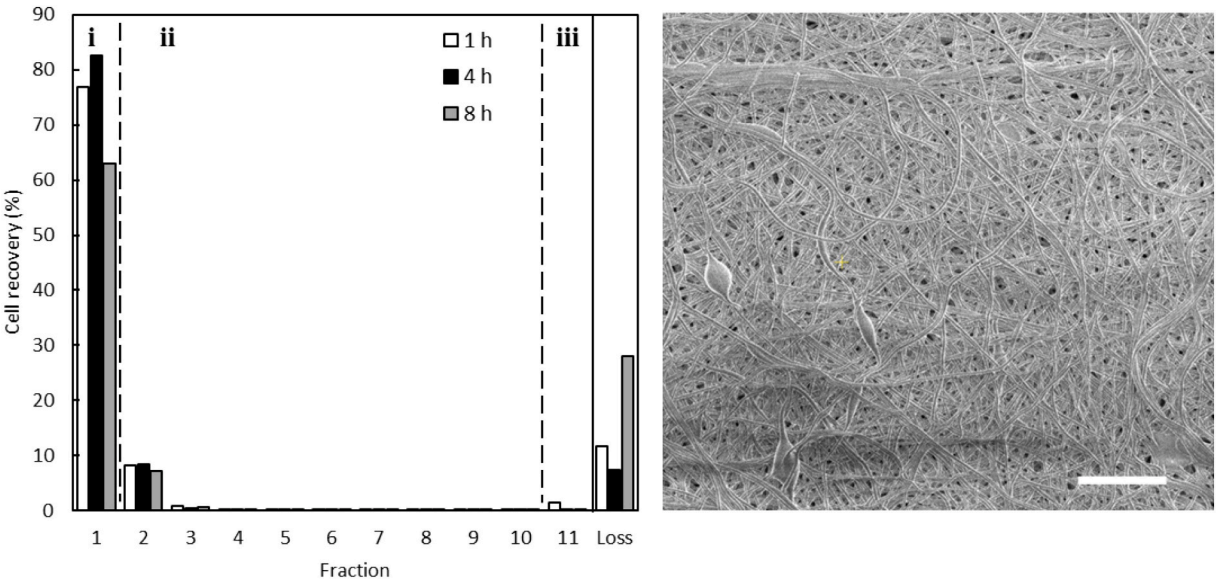

Fig. 15. Left hand side: Recovery of red blood cells (left) following flowthrough experiments through heat treated 99 % DH PVA materials produced by DC electrospinning. Phase i: initial cell challenge with sheep's blood. Phase ii: PBS forward wash. Phase iii: PBS reverse wash. The percentage of cells unaccounted for at the end of each run is indicated in the right-hand column as 'Loss' (fraction volume: 5 mL). Key: 1 h heat treated membranes (white); 4 h (black); 8 h (grey). Right hand side: SEM image of a membrane treated for 4 h after flowthrough experiments and cell fixing (scale bar: 10 μm).

observed for all the membranes, with most cells being recovered in fractions 2 and 3. Cells recovered in phase *ii* (fraction 'R'), suggest a small degree of caking on the filter, though cell counts indicate that this makes up for <6 % of all recovered cells in all three experiments. Final wash steps at increased flow rates (phase *iii*) were intended to flush residual cells from the system. It seems that most cells (>70 %) were able to pass freely through the membranes under normal operating conditions, despite the apparent tight packing of the nanofibers. The total combined cell recoveries from membranes treated for 1, 4 and 8 h were 78.55 %, 77.93 % and 83.08 % respectively. This suggests that even after thorough flushing, the overall loss to the system is on average 20.15 %. It was however unclear if this percentage would be consistent regardless of scale of the cell challenge, and whether it would ultimately lead to the clogging of the membrane.

To test the membrane performance in the presence of blood, pure defibrinated sheep's blood (a screened mammalian blood product with coagulating components removed) was employed during subsequent cell permeation experiments. Defibrinated sheep's blood contains approximately 10^{10} cells per mL, and such large cell volumes would highlight any membrane clogging issues. The erythrocytes themselves have a similar morphology to human RBCs, with an average diameter of up to 4.5 μm, compared to 7 μm for human RBCs [85,88]. The percentage of cells recovered in each fraction (5 mL fraction volume) is based on the number of cells in the initial feedstock and are shown in Fig. 15 (left hand side graph). Most cells were collected in the first two fractions (62.9 %–81.7 % in the first one and 7.2–8.3 % in the second), whereas all other fractions contained no more than 0.8 % of the initial cell challenge. Cumulative cell counts indicate that in total 88.4 %, 92.7 %, and 71.9 % of cells were accounted for, from the non-woven mats that were heat treated for 1 h, 4 h and 8 h, respectively. To find out if the cells lost in the system were physically trapped or non-specifically bound to the polymeric network, a representative membrane was immersed in formaldehyde (to fix any entrapped cells), lightly rinsed with PBS, and analysed by ESEM. The image from the 4 h heat treated sample (Fig. 15, right hand side) shows no sign of entrapped RBCs or any other large entities. Although it seems possible that there could be flow restrictions through the small pore sizes observed in the ESEM image, the RBCs are clearly able to migrate through the network. This is not surprising based on their morphology and function. Erythrocytes can travel through 3–5 μm capillaries and 0.5–1 μm splenic sinuses during their lifespan [89,90], because of their ability to undergo cellular deformation. This, combined with the added flexibility of the individual polymeric fibres, which allows them to also deform around the cells during flow, results in the unimpeded passage of RBCs through pores that are seemingly much smaller than the cells themselves. Given the absence of cells observed within the membrane, the apparent loss is considered a limitation of the traditional cell counting method, which is subject to human error in both dilution and counting steps - a problem which is enhanced further when handling highly concentrated suspensions. Future work will look to address this by utilising hydrodynamically focused impedance measurements for counting RBCs.

4. Conclusion

The aim of this research was to assess the suitability of heat stabilized electrospun PVA non-woven materials for blood processing, as part of a proposed alternative blood salvage platform. Largely defect-free, nanofibrous membranes were successfully produced by two different electrospinning methods using highly hydrolysed PVA feedstocks. These membranes were stabilized by heat treatment at 180 °C and the duration of heating influenced material characteristics, including swelling, leaching behaviour and mechanical properties. There was a positive correlation between the length of heat treatment and the preservation of the non-woven fibrous morphology of the supports following contact with water, which indicated an enhanced level of cross-linking with increased heating time. Through tensile testing, it was observed that samples produced using the higher degree of hydrolysis PVA (*i.e.* 99 %) resulted in materials with greater UTS across all heat treatment durations when compared to untreated ones, and these samples were therefore carried forward for further experiments on the effect of the electrospinning method. FT-IR indicated no characteristic change in the chemical structure between DC and AC electrospun mats but did demonstrate that materials which were subjected to heat treatments had increased physical crosslinking, as well as some degree of chemical crosslinking. Heat treatment for longer times caused thermal degradation by scission and polyene formation. Cytotoxicity testing using the extract method confirmed that regardless of electrospinning method employed and heat treatment duration, potential leachables generated from the dissolution of the PVA membranes had no deleterious effect on cell viability. AC electrospinning generated a very open fibrous network, but since this production method is still in its infancy with regards to scale-up potential and GMP operation, DC electrospun supports were chosen for subsequent cell flowthrough experiments. Though further optimization is required, in all cases, and for both low and high cell concentrations, the majority of cells successfully permeated the membranes, which confirms the inert open pore structure of these materials and therefore their suitability as base matrices in membrane chromatography for cell processing applications. Next steps currently under way in our laboratories involve the attachment of immunoaffinity ligands to the PVA backbone, followed by the selective removal of target cells from model bi-cellular suspensions. In parallel, we are also exploring the very promising AC electrospinning technology platform, which appears to deliver the very large pores necessary for the processing of big biological entities, such as human cells.

Author agreement

This is to certify that all authors have seen and approved the final version of the manuscript being submitted. They warrant that the article is the authors' original work, hasn't received prior publication and isn't under consideration for publication elsewhere.

Declaration of competing interest

The authors declare the following financial interests/personal relationships which may be considered as potential competing interests:

Eirini Theodosiou reports financial support was provided by The Royal Society. Eirini Theodosiou reports financial support was provided by The Birmingham Orthopaedic Charity. Vera Jencova reports financial support was provided by The Czech Health Research Council.

Data availability

Data will be made available on request.

Acknowledgements

This work was supported by the Royal Society International Exchanges grant IES\R3\183098, the Birmingham Orthopaedic Charity, and the Czech Health Research Council project No NV18-01-00332. WJAH would like to thank Dr. Petra Hanga and Megan Boseley for providing the hMSCs for cytotoxicity tests, Dr. Eric Hill and David Jenkins for supplying the SH-SY5Y cell line for flowthrough experiments, and Jakub Sacharczuk for his help with the ESEM. The authors would also like to thank Benjamin Dagès for drawing Figs. 1 and 12(a).

Appendix A. Supplementary data

Supplementary data to this article can be found online at https://doi.org/10.1016/j.bioadv.2022.213197.

References

[1] G. Shulman, Quality of processed blood for autotransfusion, J. Extra Corpor. Technol. 32 (2000) 11–19.
[2] Y. Chen, et al., Blood loss in spinal tumour surgery and surgery for metastatic spinal disease a META-ANALYSIS, Bone Joint J. 95B (5) (2013) 683–688.
[3] S. Jaramillo, et al., Perioperative blood loss: estimation of blood volume loss or haemoglobin mass loss? Blood Transfus. 18 (1) (2020) 20–29.
[4] UK Government, in: NHSBT (Ed.), NHS Blood and Transplant Annual Report and Accounts: 2017 to 2018, Her Majesty's Stationery Office, UK, 2018.
[5] UK Government, in: NHSBT (Ed.), NHS Blood and Transplant Annual Report and Accounts: 2018 to 2019, Her Majesty's Stationery Office, UK, 2019.
[6] UK Government, in: NHSBT (Ed.), NHS Blood and Transplant Annual Report and Accounts: 2019 to 2020, Her Majesty's Stationery Office, UK, 2020.
[7] M. Chasse, et al., Effect of blood donor characteristics on transfusion outcomes: a systematic review and meta-analysis, Transfus. Med. Rev. 30 (2) (2016) 69–80.
[8] E.C. Vamvakas, M.A. Blajchman, Transfusion-related mortality: the ongoing risks of allogeneic blood transfusion and the available strategies for their prevention, Blood 113 (15) (2009) 3406–3417.
[9] A. Shander, et al., Patient blood management – the new frontier, Best Pract. Res. Clin. Anaesthesiol. 27 (1) (2013) 5–10.
[10] G.M. Liumbruno, et al., Patient blood management: a fresh look at a fresh approach to blood transfusion, Minerva Anestesiol. 81 (10) (2015) 1127–1137.
[11] R.A. Sikorski, et al., Autologous blood salvage in the era of patient blood management, Vox Sang. 112 (6) (2017) 499–510.
[12] S.M. Frank, et al., Clinical utility of autologous salvaged blood: a review, J. Gastrointest. Surg. 24 (2) (2020) 464–472.
[13] D.R. Spahn, A. Shander, A. Hofmann, The chiasm: transfusion practice versus patient blood management, Best Pract. Res. Clin. Anaesthesiol. 27 (1) (2013) 37–42.
[14] J.P. Isbister, The three-pillar matrix of patient blood management, No S1, in: State of the Art Presentations 33rd International Congress of the International Society of Blood Transfusion, in Conjunction with the 33rd Congress of the Ksbt and 2014 Congress of the Korean Hematology Societies Vol 10, 2015, pp. 286–294, 10(S1).
[15] A.S. Zaw, et al., Metastatic spine tumor surgery: does perioperative blood transfusion influence postoperative complications? Transfusion 57 (11) (2017) 2790–2798.
[16] D. Fischer, et al., Red blood cell transfusion and its alternatives in oncologic surgery-a critical evaluation, Crit. Rev. Oncol. Hematol. 134 (2019) 1–9.
[17] SorinGroup, The eXtraordinarily Innovative, Intuitive and Powerful ATS System, 2013.
[18] AdvancisSurgical, HemoSep: Cell Saver for All Blood Components, Nottinghamshire, England, 2017.
[19] Haemonetics, Cell Saver® 5+ Brochure, 2019. Massachusetts: USA.
[20] Fresenius Kabi, CATSmart: procedures [cited 2020 April 16th]; Available from, https://www.fresenius-kabi.com/in/products/catsmart, 2020.
[21] JPAC, Information on ICS Equipment, 2020 [cited 2020 04/02/20]; List of IOCS manufacturers]. Available from: <Go to WoS>://WOS:000319335400053.
[22] N. Kumar, et al., Metastatic efficiency of tumour cells can be impaired by intraoperative cell salvage process: truth or conjecture? Transfus. Med. 27 (Suppl. 5) (2017) 327–334.
[23] V. Akpe, et al., Circulating tumour cells: a broad perspective, J. R. Soc. Interface 17 (168) (2020).
[24] F. Miyazono, et al., Surgical maneuvers enhance molecular detection of circulating tumor cells during gastric cancer surgery, Ann. Surg. 233 (2) (2001) 189–194.
[25] J.R. Marshall, M.R. King, Surgical intervention and circulating tumor cell count: a commentary, Transl. Cancer Res. 5 (2016) S126–S128.
[26] P. Perseghin, et al., Effectiveness of leukocyte filters in reducing tumor cell contamination after intraoperative blood salvage in lung cancer patients, Vox Sang. 72 (4) (1997) 221–224.
[27] R.C.G. Martin, et al., Evaluation of intraoperative autotransfusion filtration for hepatectomy and pancreatectomy, Ann. Surg. Oncol. 12 (12) (2005) 1017–1024.
[28] S. Catling, et al., Use of a leucocyte filter to remove tumour cells from intra-operative cell salvage blood, Anaesthesia 63 (12) (2008) 1332–1338.
[29] M. Poli, et al., Intraoperative autologous blood recovery in prostate cancer surgery: in vivo validation using a tumour marker, Vox Sang. 95 (4) (2008) 308–312.
[30] R.B. Rajasekaran, et al., The role of intraoperative cell salvage for musculoskeletal sarcoma surgery, J. Bone Oncol. (2021) 30.
[31] J.H. Waters, et al., Blood salvage and cancer surgery: a meta-analysis of available studies, Transfusion 52 (10) (2012) 2167–2173.
[32] A.A. Klein, et al., Association of Anaesthetists guidelines: cell salvage for peri-operative blood conservation 2018, Anaesthesia 73 (9) (2018) 1141–1150.
[33] J. Curling, Process Chromatography: Five Decades of Innovation, 2007 [cited 2021 11th of August].
[34] F. Mohr, et al., Efficient immunoaffinity chromatography of lymphocytes directly from whole blood, Sci. Rep. (2018) 8.
[35] M.B. Dainiak, et al., Cell chromatography: separation of different microbial cells using IMAC supermacroporous monolithic columns, Biotechnol. Prog. 21 (2) (2005) 644–649.
[36] A. Kumar, A. Srivastava, Cell separation using cryogel-based affinity chromatography, Nat. Protoc. 5 (11) (2010) 1737–1747.
[37] M. González-González, et al., Monolithic chromatography: insights and practical perspectives, J. Chem. Technol. Biotechnol. 92 (1) (2017) 9–13.
[38] P. Gagnon, Monoliths seen to revitalize bioseparations - new research will broaden the range of applications, Genet. Eng. News 26 (17) (2006).
[39] V. Orr, et al., Recent advances in bioprocessing application of membrane chromatography, Biotechnol. Adv. 31 (4) (2013) 450–465.
[40] K. Aliko , et al., Poly(butylene succinate) fibrous dressings containing natural antimicrobial agents. J. Ind. Text..
[41] B. Diez, et al., Chemically cross-linked poly(vinyl alcohol) electrospun fibrous mats as wound dressing materials, J. Chem. Technol. Biotechnol. 97 (3) (2022) 620–632.
[42] K. Javed, et al., A method for producing conductive graphene biopolymer nanofibrous fabrics by exploitation of an ionic liquid dispersant in electrospinning, Carbon 140 (2018) 148–156.
[43] J.-C. Park, et al., Electrospun poly(vinyl alcohol) nanofibers: effects of degree of hydrolysis and enhanced water stability, Polym. J. 42 (3) (2010) 273–276.
[44] Q.B. Yang, et al., Influence of solvents on the formation of ultrathin uniform poly (vinyl pyrrolidone) nanofibers with electrospinning, J. Polym. Sci. B Polym. Phys. 42 (20) (2004) 3721–3726.
[45] O. Hardick, et al., Nanofiber adsorbents for high productivity downstream processing, Biotechnol. Bioeng. 110 (4) (2013) 1119–1128.
[46] O. Hardick, et al., Nanofiber adsorbents for high productivity continuous downstream processing, J. Biotechnol. 213 (2015) 74–82.
[47] K. Fujimoto, M. Minato, Y. Ikada, Poly(vinyl alcohol) hydrogels prepared under different annealing conditions and their interactions with blood components, Polym. Biol. Biomed. Significance 540 (1994) 228–242.
[48] A.K. Bajpai, R. Saini, Designing of macroporous biocompatible cryogels of PVA-haemoglobin and their water sorption study, J. Mater. Sci. Mater. Med. 20 (10) (2009) 2063–2074.
[49] N. Alexandre, et al., Biocompatibility and hemocompatibility of polyvinyl alcohol hydrogel used for vascular grafting-in vitro and in vivo studies, J. Biomed. Mater. Res. A 102 (12) (2014) 4262–4275.
[50] M. Teodorescu, M. Bercea, S. Morariu, Biomaterials of PVA and PVP in medical and pharmaceutical applications: perspectives and challenges, Biotechnol. Adv. 37 (1) (2019) 109–131.
[51] A. Kumar, S.S. Han, PVA-based hydrogels for tissue engineering: a review, Int. J. Polym. Mater. Polym. Biomater. 66 (4) (2017) 159–182.
[52] S. Khazaei, S.A. Mozaffari, F. Ebrahimi, Polyvinyl alcohol as a crucial omissible polymer to fabricate an impedimetric glucose biosensor based on hierarchical 3D-NPZnO/chitosan, Carbohydr. Polym. 266 (2021), 118105.
[53] Y. Deng, et al., Morphology engineering processed nanofibrous membranes with secondary structure for high-performance air filtration, Sep. Purif. Technol. 294 (2022).
[54] Y. Deng, et al., Multi-hierarchical nanofiber membrane with typical curved-ribbon structure fabricated by green electrospinning for efficient, breathable and sustainable air filtration, J. Membr. Sci. 660 (2022), 120857.
[55] G.T. Hermanson, A.K. Mallia, P.K. Smith, Immobilized Affinity Ligand Techniques, Academic Press, 1992.
[56] T. Šutar, New Formats for Affinity Selection of Human Therapeutic Cells, Loughbourough University, 2015.
[57] A. Koski, K. Yim, S. Shivkumar, Effect of molecular weight on fibrous PVA produced by electrospinning, Mater. Lett. 58 (3–4) (2004) 493–497.
[58] P. Supaphol, S. Chuangchote, On the electrospinning of poly(vinyl alcohol) nanofiber mats: a revisit, J. Appl. Polym. Sci. 108 (2) (2008) 969–978.
[59] L. Yao, et al., Electrospinning and stabilization of fully hydrolyzed poly(vinyl alcohol) fibers, Chem. Mater. 15 (9) (2003) 1860–1864.
[60] B. Koprivova, et al., Large-scale electrospinning of poly (vinylalcohol) nanofibers incorporated with platelet-derived growth factors, Express Polym Lett 14 (10) (2020) 987–1000.
[61] X. Yang, et al., Thermal and rheological properties of poly(vinyl alcohol) and water-soluble chitosan hydrogels prepared by a combination of γ-ray irradiation and freeze thawing, J. Appl. Polym. Sci. 109 (6) (2008) 3825–3830.
[62] O.N. Tretinnikov, S.A. Zagorskaya, Determination of the degree of crystallinity of poly(vinyl alcohol) by FT-IR spectroscopy, J. Appl. Spectrosc. 79 (4) (2012) 521–526.
[63] M. Miraftab, A.N. Saifullah, A. Çay, Physical stabilisation of electrospun poly(vinyl alcohol) nanofibres: comparative study on methanol and heat-based crosslinking, J. Mater. Sci. 50 (4) (2014) 1943–1957.
[64] M.S. Enayati, et al., Crystallinity study of electrospun poly (vinyl alcohol) nanofibers: effect of electrospinning, filler incorporation, and heat treatment, Iran. Polym. J. 25 (7) (2016) 647–659.
[65] T.A.W. Wijanarko, Effect of Heat Treatment on Morphology and Crystallinity of Electrospun Poly(vinyl Alcohol) Nanofibers, 2016.
[66] D. Kharaghani, et al., Design and characterization of dual drug delivery based on in-situ assembled PVA/PAN core-shell nanofibers for wound dressing application, Sci. Rep. 9 (1) (2019) 12640.
[67] J.H. George, et al., A closer look at neuron interaction with track-etched microporous membranes, Sci. Rep. (2018) 8.
[68] J. Valtera, et al., Fabrication of dual-functional composite yarns with a nanofibrous envelope using high throughput AC needleless and collectorless electrospinning, Sci. Rep. 9 (1) (2019) 1801.
[69] I. Restrepo, et al., The effect of molecular weight and hydrolysis degree of poly (vinyl alcohol)(PVA) on the thermal and mechanical properties of poly(lactic acid)/PVA blends, Polimeros Cienc. Tecnol. 28 (2) (2018) 169–177.
[70] S.T. Lin, et al., Anti-fatigue-fracture hydrogels, Sci. Adv. 5 (2019) 1.
[71] H.G. Yang, et al., Thermal decomposition behavior of poly (vinyl alcohol) with different hydroxyl content, J. Macromol. Sci. Part B Phys. 51 (1–3) (2012) 464–480.
[72] Y.F. Gao, et al., A mechanistic interpretation of the strength-ductility trade-off and synergy in lamellar microstructures, Mater. Today Adv. (2020) 8.

[73] M. Najafiasl, et al., Modeling of drug release and simultaneous enhancement of tensile strength and antioxidant activity of the electrospun nanofibres using naturally extracted oil from Pistacia atlantica, Polym. Test. 107 (2022).
[74] S.R. Dods, et al., Fabricating electrospun cellulose nanofibre adsorbents for ion-exchange chromatography, J. Chromatogr. A 1376 (2015) 74–83.
[75] K. Chen, K.S. Schweizer, Theory of yielding, strain softening, and steady plastic flow in polymer glasses under constant strain rate deformation, Macromolecules 44 (10) (2011) 3988–4000.
[76] C.M. Tang, Y.H. Tian, S.H. Hsu, Poly(vinyl alcohol) nanocomposites reinforced with bamboo charcoal nanoparticles: mineralization behavior and characterization, Materials 8 (8) (2015) 4895–4911.
[77] H. Lee, B. Park, H. Kim, Crystallinity and diameter changes of electrospun fiber for different processing conditions and collection areas, Text. Sci. Eng. (2012) 49.
[78] S.N. Alhosseini, et al., Synthesis and characterization of electrospun polyvinyl alcohol nanofibrous scaffolds modified by blending with chitosan for neural tissue engineering, Int. J. Nanomedicine 7 (2012) 25–34.
[79] I.M. Jipa, et al., Effect of gamma irradiation on biopolymer composite films of poly (vinyl alcohol) and bacterial cellulose, Nucl. Inst. Methods Phys. Res. B 278 (2012) 82–87.
[80] H.S. Mansur, et al., FTIR spectroscopy characterization of poly (vinyl alcohol) hydrogel with different hydrolysis degree and chemically crosslinked with glutaraldehyde, Mater. Sci. Eng. C Biomim. Supramol. Syst. 28 (4) (2008) 539–548.
[81] J.Q. Han, et al., Electrospun Core-Shell nanofibrous membranes with nanocellulose-stabilized carbon nanotubes for use as high-performance flexible supercapacitor electrodes with enhanced water resistance, thermal stability, and mechanical toughness, ACS Appl. Mater. Interfaces 11 (47) (2019) 44624–44635.
[82] A.A. Sapalidis, Porous polyvinyl alcohol membranes: preparation methods and applications, Symmetry-Basel 12 (6) (2020).
[83] G. Meszlényi, G. Körtvélyessy, Direct determination of vinyl acetate content of ethylene-vinyl acetate copolymers in thick films by infrared spectroscopy, Polym. Test. 18 (7) (1999) 551–557.
[84] H.S. Baek, et al., Evaluation of the extraction method for the cytotoxicity testing of latex gloves, Yonsei Med. J. 46 (4) (2005) 579–583.
[85] J.M. Ward, 19 - hematopoietic and lymphoid tissues, in: Comparative Anatomy and Histology, Second Edition, Academic Press, San Diego, 2018, pp. 365–401.
[86] T. Nelson, et al., Electrospun composite polycaprolactone scaffolds for optimized tissue regeneration, Proc. Inst. Mech. Eng. Part N: J. Nanoengineering Nanosystems 226 (2012) 111–121.
[87] Elmarco, NS 8S1600U: scalable industrial production line. https://www.elmarco.com/production-lines/ns-8s1600u, 2020 [cited 2021 11th of August].
[88] N. Adili, M. Melizi, H. Belabbas, Species determination using the red blood cells morphometry in domestic animals, Vet. World 9 (9) (2016) 960–963.
[89] G. Tomaiuolo, Biomechanical properties of red blood cells in health and disease towards microfluidics, Biomicrofluidics 8 (5) (2014).
[90] P. Brånemark, J. Lindström, Shape of circulating blood corpuscles, Biorheology 1 (1963) 139–142.